2005 WSEAS Int. Conf. on REMOTE SENSING, Venice, Italy, November 2-4, 2005 (pp55-60)

Study of cloud-clearing error versus footprint size using aircraft NAST-I infrared sounder observations

V. V. ZAVYALOV, G. E. BINGHAM, D. K. ZHOU*, C. GOING, M. SMITH, AND J. MORRIS
Space Dynamics Laboratory, USURF, Logan, UT 84341-1942, USA
* Atmospheric Sciences, NASA Langley Research Center, Hampton, VA, USA

Abstract: - The airborne NPOESS Aircraft Sounding Test-bed-Interferometer (NAST-I) instrument has been developed to collect controlled sets of very high quality spectral radiance and retrieved atmospheric profile reference data. This data is used to validate the spacecraft radiance measurements and derived geophysical products. NAST-I data is also used to support the development and performance validation of high spectral resolution spectrometers as well as for testing inversion methods and approaches. The NAST-I instrument's high spatial resolution makes it possible to conduct retrieval error analysis with respect to sampling area. This paper studies the relationship between the size of the NAST-I sensor sampling area and the errors induced by the retrieval process using both clear column and cloud contaminated radiances. The traditional single-band N* cloud-clearing technique is used to extrapolate to a cloud free value the radiances observed in two adjacent fields of view, which have differing cloud content. Temperature profile retrievals based on clear and cloud-cleared radiances are then analyzed with respect to the NAST-I footprint size. Remarkable differences are observed for clear and cloud-cleared sampling areas. Increasing the footprint size causes the cloud contaminated areas to have a significant amplification of temperature errors with respect to radiosonde data. On the other hand, clear sky retrieval errors decrease, which then exhibit a more typical behavior for radiance errors induced by instrument noise.

Key-Words: Remote sensing, IR measurements, spectroscopy, cloud contamination, cloud-clearing

1 Introduction

The advanced infrared sounding instruments developed for operational weather and climate satellites provide the high-spectral and spatial resolution radiance data needed to improve the accuracy of space-based temperature and moisture profiles. Clouds have a significant effect on satellite observed infrared radiances, which limits the ability of these observations to be assimilated in numerical weather forecast models [1]. Several techniques have been developed to deal with cloud contaminated FOVs (fields of view) including "hole-hunting" and "cloud-clearing" schemes. Clear sky radiances and retrievals are the most straightforward way of using satellite observations. These observations are used for scientific studies, calibration/validation programs, and for operational data being included in weather forecast and climatology models. Three years of flight observations from AIRS (Atmospheric InfraRed Sounder) and AMSU (Advanced Microwave Sounding Unit) have shown that the total cloud free yields of AMSU FOVs are globally less than 15-20% [2, 3]. These results agree well with the optimal spatial resolution study conducted by H.-L. Huang et al. [4]. In this study a 1-km MODIS imager cloud mask was used to analyze the probability of finding a fully cloud free sampling area within a single AMSU FOV. It was shown that reducing the AIRS FOV size significantly increased the yield of sampled areas for which clear sounding retrievals can be performed.

Approaches used by "cloud-clearing" algorithms attempt to obtain clear profiles for

sounding, which are in close proximity to the cloud. These profiles are then used to fill in a nearby cloud field so as to improve the "clear" data yield for weather forecast model assimilation. The cloud-clearing is not required to accurately model a cloud's physical and optical properties. This approach is now widely used to retrieve geophysical parameters of the atmosphere in presence of semi-transparent clouds [2, 5, 6]. Cloud-clearing approaches allow a significant increase in the overall yield of sampling areas for which cloud-free or reliably cloud-cleared sounding retrievals can be performed. For instance, the AIRS team cloud-clearing approach allows an increase in the overall yield of clear and cloud-cleared soundings of up to 50-70% [3].

Cloud-clearing error versus high spectral resolution infrared sensor footprint size has been studied by Arnesen et al. [7] using actual atmospheric data collected by the NPOESS Aircraft Sounding Testbed Interferometer (NAST-I). Results of this study show that the decrease in FOV size reduces the cloud-clearing error independently of the sampling average configuration. This general result is obtained by analyzing the spectral differences between the mean radiances of the "truth" and an "estimate" of the reduced resolution data obtained by the linear combination of the FOVs performed before and after the cloud-clearing procedure respectively [7].

In this paper the results of this study are extended by analyzing the retrieved temperature profiles as compared to the reference "truth" profiles such as collocated dropsonde and radiosonde data. The retrieval algorithm consists of two major parts. The first is the cloud-clearing part of the algorithm which is based on the traditional N* cloud-clearing technique [5, 7]. This is used to estimate the clear column radiance measurements from the observations over partly cloudy regions. The second is the eigenvector regression retrieval method [8] to retrieve temperature and water vapor profiles using clear sky and cloud-cleared radiances. The statistics and final results are analyzed separately for clear sky and cloud-cleared retrievals.

2 Statistics.

In this study ten NAST-I flights described previously (see Table 1 in [7]) were used to generate statistics of clear sky and cloud-cleared FOVs. They include the CAMEX (08/26/98 and 09/22/98), WINTEX (03/20/99), Wallops Ferry (08/27/99), W. Pacific (03/08/01, 03/09/01, 03/10/01, 03/12/01, 03/16/01), CLAMS (07/12/01), and Crystal Face (07/26/02, 07/29/02) campaigns. A generic cloud mask algorithm is used to classify each footprint of each resolution as clear or cloud contaminated. A FOV is classified as clear if it passes a three point test:

A. $|\Delta BT| \leq 2.0K$ for the 11 and 12 μm windows, and

B. $|\Delta BT| \leq 2.0K$ for the 11 and 10 μm windows, and

C. Mean BT for the 894 - 904 cm-1 window of ≥ 294 K.

ΔBT is a brightness temperature difference between two window channels. A reduced resolution FOV is considered cloudy if within it at least one full resolution FOV is determined as cloudy.

Overall statistics for all ten campaigns are shown in Fig. 1.

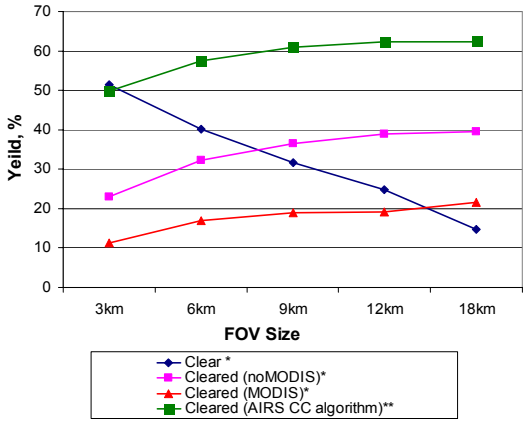

Fig.1. Overall yield of clear and cloud-cleared FOV over several NAST-I flights versus FOV size.

The blue diamonds represent the total percentage of clear sky radiances for full (~2.6 km at nadir) and reduced resolution FOVs (from 6 to 18 km at nadir) over all ten NAST-I flights. The yield of clear FOVs with reduced

resolution drops dramatically from 54% for full resolution FOVs to 21% for 13.5 km of AIRS FOV size at the nadir. These results are in agreement with AIRS observations [3] and the optimal spatial resolution study [4] mentioned previously.

The other three lines on Fig. 1 represent the overall percentage of cloud contaminated FOVs that were accepted for cloud-clearing with the traditional N* algorithm described previously (crimson squares and orange triangles) and with AIRS cloud-clearing algorithm (green squares). The crimson curve was generated with additional constraint applied to the cloud-cleared radiances. It limits the absolute radiance value of cloud-cleared FOVs to be within 1% of mean absolute value of nearby clear sky radiances (simulation of MODIS filter [7]). The AIRS cloud-clearing approach was implemented by our group to explore performance of this algorithm with application to the NAST-I data. This advanced algorithm is able to handle multiple cloud formations [2] and shows almost twice the yield of cloud-cleared FOVs as compared to the traditional N* approach (see Fig. 1).

The yield of cloud-cleared FOVs slightly increases with the increase in FOV size. When reduced resolution FOVs are assembled from the full resolution FOVs, the probability of cloud contamination increases and the relative number of cloud contaminated FOVs also increases. Reduced resolution FOVs may be assembled from clear and cloud contaminated full resolution FOVs so that the reduced resolution FOVs become semitransparent and would be acceptable for cloud-clearing. This leads to the increase in total yield of cloud-cleared FOVs.

Cloud-clearing significantly increases overall yield of FOVs accepted for retrievals from 20% of clear cases to 60-82% of clear and cloud-cleared cases with respect to a 13.5 km AIRS footprint size. The total yield of clear and cloud-cleared FOVs slightly decreases with the increase in the FOV size from 76% (3 km resolution) to 60% (13.5 km resolution) in a case of N* algorithm and from almost 100% to 82% in a case of AIRS cloud-clearing approach.

3 Observation angle errors

The cloud-clearing algorithms assume that the observed NAST-I footprints differ one from another only in the cloud amount. The N* algorithm as well does not take into account the difference in view angles of adjacent FOVs which were chosen for estimation of the N* correction parameter. To account for the view angle difference between adjacent FOVs, a local angle correction (LAC) procedure should be performed before attempting any cloud-clearing procedure. The NOAA approach [9] appears to be the most efficient way to perform LAC. This procedure is based on synthetic regression, trained on a wide range of cloud conditions and profiles that cover the expected atmospheric range.

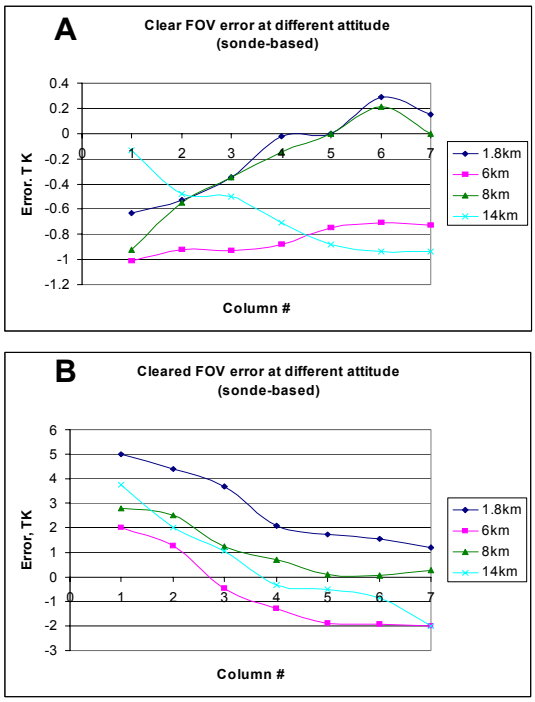

Fig.2 Retrieval temperature biases versus view angle (column #) for clear (A) and cloud-cleared FOVs (B).

Another possible approach for cloud-clearing study is to use only FOVs that are close to the nadir. In Fig.2 retrieval temperature biases against collocated radiosonde profiles are shown as a function of the view angle (column #) for clear and cloud-cleared FOVs

separately. These biases are shown as slices at different altitudes ranging from the surface to 14 km. For this and further studies, we use the N* cloud clearing algorithm and data from the Crystal Face NAST-I flight over the West Atlantic Ocean.

It is seen in Fig.2A that for all altitudes the clear FOV retrievals exhibit no significant bias dependence on the view angle. This means that the retrieval algorithm properly handles view angle dependencies. On the other hand, the cloud-cleared FOV retrievals exhibit large systematic biases depending on the view angle as shown in Fig.2B. It is evident that these biases are induced by the cloud-clearing procedure being performed without any LAC. Nevertheless, biases induced along the nadir are relatively small, with negligible dependence on view angle; therefore, they can be used to study relative errors in cloud-clearing procedure.

4 Retrieval errors versus FOV size

When the clear column or cloud-cleared radiances are formed as a linear combination of the radiances of different FOVs, the effect of instrument noise will be amplified from a single FOV noise [2]:

$$\delta R_n = NEdN_n \cdot A_n \qquad (1)$$

Where $A_n = 1/(N_F)^{1/2}$ for averaged clear channels, when instrumental noise $NEdN_n$ is dominant, and $A_n = A_\eta$ is a noise amplification factor caused by the cloud-clearing procedure. N_F is the number of FOVs averaged to produce a reduced resolution FOV. The noise in the measured radiances propagates to the final retrieval of temperature and can be expressed for each altitude level by the following:

$$\delta T = \sum (dT / dRn) \cdot \delta Rn \cdot An \qquad (2)$$

For clear column retrievals, the temperature retrieval error normalized by the error of the full resolution FOV ($\delta T_{NF=1}$) can be expressed as:

$$(\delta T_{NF} / \delta T_{NF=1})^2 = 1/N_F \qquad (3)$$

For cloud-cleared FOVs, the normalized error is proportional to the ratio of noise amplification factors of both reduced ($A_{\eta NF}$) and full resolution ($A_{\eta NF=1}$) FOVs:

$$(\delta T_{NF} / \delta T_{NF=1})^2 \sim (A_{\eta NF} / A_{\eta NF=1})^2 \qquad (4)$$

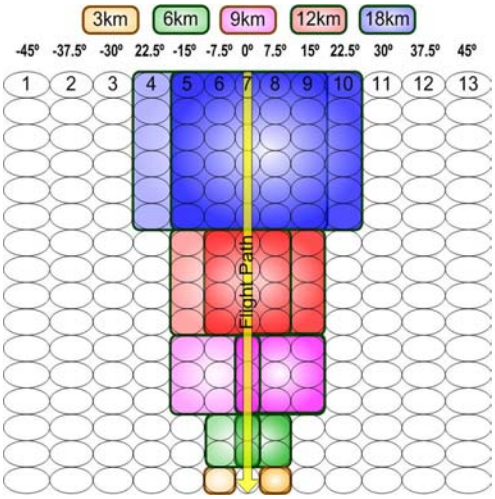

Fig.3. Illustration of the averaging method used to simulate reduced resolution FOVs along the nadir.

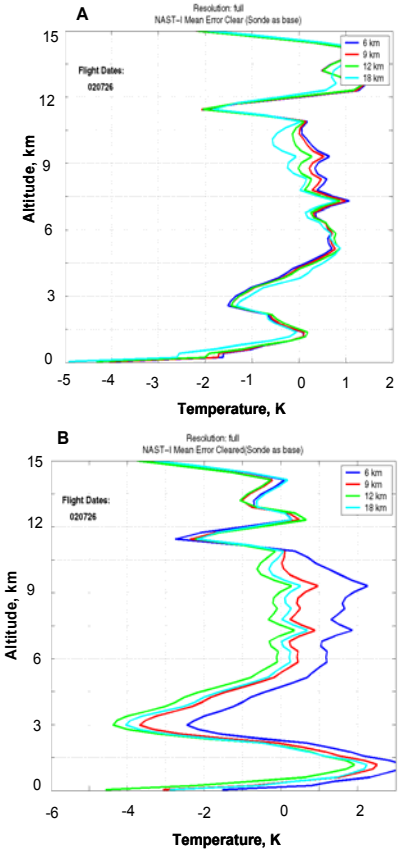

Fig.4. Temperature biases for clear (A) and cloud-cleared (B) retrievals with respect to collocated radiosonde temperature profile.

According to the above discussion, this study is conducted for reduced and full resolution FOVs assembled only along the nadir as shown in Fig. 3. Symmetrical pairs of

FOVs along the nadir for each spatial resolution are chosen with observation angles ≤ 15^0 (columns #5-9), where the relative temperature error is small (see Fig.2). Temperature biases and SDV with respect to the collocated radiosonde profiles are calculated for the Crystal Face NAST-I flight on 07/26/02.

Vertical temperature biases are shown in Fig. 4 for each reduced resolution FOV (6, 9, 12, and 18 km).

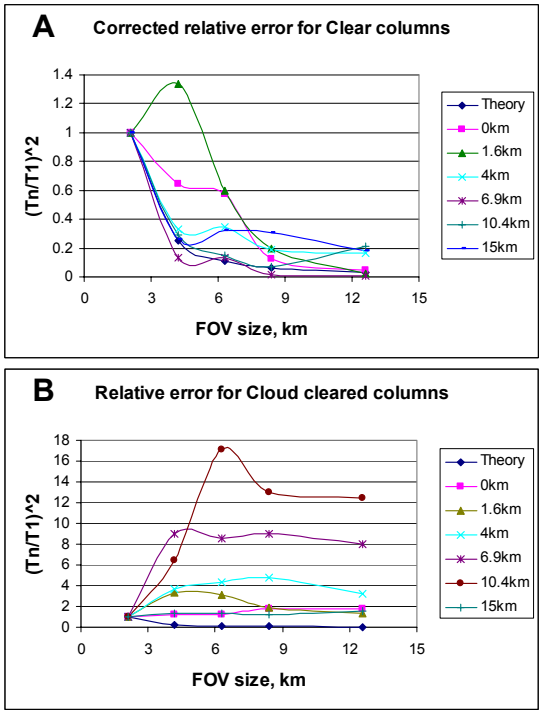

Fig.5. Temperature retrieval error amplification versus FOV size for clear (A) and cloud-cleared (B) radiances.

The normalized error amplification factor or the SDV error of temperature retrievals, as normalized according to the expressions (3) and (4) are shown in Fig. 5. The error amplification factor is shown for several altitude slices, representing large (at 0, 1.6, and 4 km) and relatively small (at 6.9, 10.4, and 15 km) temperature biases (see Fig. 4). For altitudes 0 and 4 km, large biases were removed for both clear and cloud-cleared cases according to Fig. 4, while no bias correction was performed at 1.6 km.

Remarkable difference is observed in the FOV size dependence of the error amplification factor for clear (Fig.5A) and cloud-cleared (Fig.5B) cases. For clear cases, this dependence agrees well with expression (3) indicating that instrument noise is the dominant factor in temperature retrievals. The error in clear sky retrievals decreases with an increase in FOV size, following the increase in signal-to-noise ratio (SNR). For cloud-cleared cases, the dominant source of error is the cloud-clearing procedure. The error amplification factor increases several times with the increase in FOV size for practically all altitudes, and levels off at FOV sizes larger than 6-9 km.

5 Conclusions

The National Polar-Orbiting Operational Environmental Satellite System is expected to become a central element of the long-term global observation system. Although the critical design for many sensor suites have been completed, some aspects of the configuration of these instruments can still be optimized. The trade-off between SNR, FOV size, and overall yield of satellite based retrievals is complicated and needs to be carefully considered. In this paper, we have presented the impact of FOV size on the retrieval yield statistics and retrieval errors for clear and cloud-cleared radiances based on NAST-I observations during several flight campaigns.

Our results on “hole hunting” agree well with other studies and show that decreasing FOV size significantly increases the yield of clear column cases. The accuracy of the clear sky retrievals is determined mostly by the instrument noise and increases by the factor $A_n=1/(N_F)^{1/2}$ with decreasing FOV size.

On the other hand, the yield of cloud-cleared FOVs slightly decreases with decreasing FOV size. The error amplification factor in this case is determined mostly by the cloud-clearing procedure and significantly decreases (by several times) with a decrease in sampling area size. For instance, the decrease in AIRS FOV size from 13.5 to 3 km may

reduce the errors in cloud contaminated retrievals by ~2 times, and make it comparable with clear sky retrievals. Taking into account that the total yield of clear and cloud-cleared FOVs significantly increases with a decrease in sampling area, a smaller footprint size for high spectral resolution atmospheric sounders will produce a benefit both in a higher yield of total retrievals and in improved accuracy of cloud contaminated retrievals.

To extend and verify the results of this study with more sophisticated cloud-clearing and retrieval algorithms, the AIRS/AMSU scientific algorithm has been modified by our group to provide a NAST temperature and water vapor retrieval package that works in both clear and cloudy conditions and utilizes both NAST-I interferometer and NAST-M microwave data. Preliminary results from this algorithm were reported at the 2005 CALCON Technical Conference [10].

References:

[1] Smith W. L, H. -L. Huang, and A. Jenney, An Advanced sounder cloud contamination study, *J. Appl. Meteor*., V.35, No.8, 1996, pp. 1249-1255.

[2] Susskind J., C. B. Barnet, and J. Blaisdell, Retrieval of atmospheric and surface parameters from AIRS/AMSU/HSB data in the presence of clouds, *IEEE Trans. on Geoscience and Remote Sensing,* V.41, No.2, 2003, pp. 390-409.

[3] Susskind J., C. B. Barnett, J. Blaisdell, L. Iredell, F. Keita, and L. Kouvaris, Early results from AIRS/AMSU/HSB, *Proc. SPIE Earth Observing Systems VIII*, San Diego, CA, V.5151, 2003, pp. 244-251.

[4] Huang H. -L., R. Frey, W. L. Smith, D. K. Zhou, H. Bloom, Defining Optimal Spatial Resolution for High-Spectral Resolution Infrared Sensors, *Geoscience and Remote Sensing Symposium*, 2003, IGARSS'03, *Proceedings 2003 IEEE International*., V.1, 2003, pp. 366-368.

[5] Smith W. L., An improved method for calculating tropospheric temperature and moisture profiles from satellite radiometer measurements, *Mon. Wea. Rev*., V.96, 1968, pp. 387-396.

[6] Li J., C. -Y. Liu, H. -L. Huang, T. J. Schmit, X. Wu, W. P. Manzel, and J. J. Gurka, Optimal cloud-clearing for AIRS radiances using MODIS, *IEEE Trans. on Geoscience and Remote Sensing,* V.43, No.6, 2005, pp. 1266-1278.

[7] Arnesen S. A., G. W. Cantwell, G. E. Bingham, W. L. Smith, and D. K Zhou, Cloud-clearing algorithm error vs. sensor footprint size and configuration with optional multi-spectral MODIS imagery, *Proc. SPIE Optical Spectroscopic Techniques and Instrumentation for Atmospherics and Space Research V,* San Diego, CA, V. 5157, 2003, pp. 242-252.

[8] Zhou D. K., W. L. Smith, J. Li, H. B. Howell, G. W. Cantwell, A. M. Larar, R. O. Knuteson, D. C. Tobin, H. E. Revercomb, and S. A. Mango, Thermodynamic product retrieval methodology for NAST-I and validation, Applied Optics, V.41, No.33, 2002, pp. 6,957-6,967.

[9] Goldberg M. D., Y. Qu, M. McMillin, W. Wolf, L. Zhou, and M. Divakarla, AIRS near-real-time product and algorithms is support of operational numerical weather prediction, *IEEE Trans. on Geoscience and Remote Sensing,* V.41, No.2, 2003, pp. 379-389.

[10] Smith M., C. Going, V. Zavyalov, G. Bingham, D. Zhou*, and J. Vildirim, Preliminary results of validation of satellite AIRS retrievals with aircraft NAST-I and NAST-M soundings using the same retrieval algorithm, 2005 CALCON Technical Conference, 22-25 August 2005, Logan, Utah.